Available online at www.sciencedirect.com
ScienceDirect
Journal of the European Ceramic Society 30 (2010) 2357–2364
www.elsevier.com/locate/jeurceramsoc

Improved ablation resistance of C–C composites using zirconium diboride and boron carbide☆

Erica L. Corral*, Luke S. Walker

Arizona Materials Laboratory, Materials Science and Engineering Department, The University of Arizona, 1235 East James E Rogers Way, Tucson, AZ 85721, USA

Available online 13 April 2010

Abstract

Zirconium diboride and boron carbide particles were used to improve the ablation resistance of carbon–carbon (C–C) composites at high temperature (1500 °C). Our approach combines using a precursor to ZrB_2 and processing them with B_4C particles as filler material within the C–C composite. An oxyacetylene torch test facility was used to determine ablation rates for carbon black, B_4C, and ZrB_2–B_4C filled C–C composites from 800 to 1500 °C. Ablation rates decreased by 30% when C–C composites were filled with a combination of ZrB_2–B_4C particles over carbon black and B_4C filled C–C composites. We also investigated using a sol–gel precursor method as an alternative processing route to incorporate ZrB_2 particles within C–C composites. We successfully converted ZrB_2 particles within C–C composites at relatively low temperatures (1200 °C). Our ablation results suggest that a combination of ZrB_2–B_4C particles is effective in inhibiting the oxidation of C–C composites at temperatures greater than 1500 °C.

Keywords: High-temperature materials; Precursors–organic; Sol–gel processes; Thermal properties; Composites

1. Introduction

Advanced thermal protection systems are needed to mitigate effects of aerothermal heating that otherwise limit the performance of aerospace vehicles.[1] C–C composites are a family of materials that possess extraordinary and unique characteristics that make them attractive for use in a wide range of applications especially when low density materials are desirable, such as in aerospace applications.[2–4] C–C composites have very low densities in the range of 1.5–2.2 g/cm^3 while maintaining their high mechanical strengths, >3000 MPa, at elevated temperatures in non-oxidizing environments.[4] They also have high toughness values and exhibit fracture behavior that allows them to deform gracefully under load and avoid catastrophic failure when their ultimate strengths are exceeded. They can operate in severe chemically aggressive environments but require protection from oxidation and usually use coatings or oxygen inhibitor systems[5] for continuous use above 500 °C.

Extensive research has been performed on diboride based UHTCs, such as ZrB_2 due to their extremely high melting temperatures, >3245 °C, and excellent mechanical properties at high temperature. ZrB_2 has been studied due to its low density (6.09 g/cc) and low cost. In terms of oxidation mechanisms, it has been shown that ZrB_2 oxidizes to ZrO_2 and liquid B_2O_3, which evaporates at higher temperatures (>1200 °C) as B_2O_3 (g).[6] B_4C is also one of the most stable compounds with a melting temperature of 2350 °C and very low density (2.52 g/cc).[7] Densified B_4C slowly oxidizes at 600 °C and results in the formation of a thin transparent B_2O_3 film, which cracks after cooling. Up to 1200 °C the oxidation process is limited by the diffusion of reagents through the oxide layer.[8]

Low cost and reliable testing methods for evaluating oxidation resistant materials are needed in order to investigate fundamental material oxidation mechanisms at temperature. Unfortunately, there are only a couple of test facilities that can test high-temperature materials over a wide range of temperatures, 500–2600 °C, in a controlled environment.[17] Conventional box furnaces use $MoSi_2$ heating elements that operate in air up to 1700 °C. Graphite element furnaces operate up to 2300 °C but are not capable of operating under oxidizing environments. Therefore, alternative high-temperature facilities that can operate up to 2600 °C, such oxyacetylene torches are

☆ Presented at the Air Force Office of Scientific Research Workshop on Aerospace Materials for Extreme Environments, St. Louis, MO, August 3–5, 2009.

* Corresponding author. Tel.: +1 520 621 8115; fax: +1 520 621 8059.
E-mail addresses: elcorral@email.arizona.edu, erica.corral@gmail.com (E.L. Corral).

0955-2219/$ – see front matter © 2010 Elsevier Ltd. All rights reserved.
doi:10.1016/j.jeurceramsoc.2010.02.025

critical in studying ablation and oxidation resistance of UHTCs at high-temperatures.[19]

Ablation is an erosive phenomenon with a removal of material by the combination of thermo-mechanical, thermo-chemical, and thermo-physical factors from high temperature, pressure, and velocity of combustion flame.[18] Oxidation and ablation resistance are very important properties in evaluating the utility of UHTC coatings for use in aerospace applications. The ablation behavior of diboride and carbide coatings on C–C composites and oxidation resistance of bulk UHTC composites have been successfully studied using oxyacetylene torch testing.[19]

Our approach is to use ZrB_2 and B_4C particles as inhibitors to the oxidation process of bulk C–C composites using liquid precursors and powder filled phenolic resins that are incorporated into the C–C composite fabrication steps. The liquid precursor method involves coating the C–C composite with precursors prior to composite lamination and densification. Although, there has been significant work on developing UHTC coatings for oxidation protection of carbon fibers and C–C composites[9–16] there has been limited work on developing ZrB_2 and B_4C inhibited C–C composites. The goal of this research is to investigate alternative C–C composite inhibition processing methods using precursors to ZrB_2 and investigate high-temperature oxidation and ablation testing methods using oxyacetylene torch testing on commercially available B_4C filled C–C composites.

2. Experimental procedure

2.1. C–C composite materials and processing

The C–C composite supplier (HITCO Carbon Composites Inc., Gardenia, CA) performed multiple variations of C–C processing and post-processing heat treatments per our request. Composite compositions were varied based on the whether or not the phenolic resin was filled with 30 wt.% B_4C particles, conventional carbon black, or ZrB_2–B_4C particles. A list of the processing conditions and properties measured at HITCO for the samples they supplied are shown in Table 1. The carbon black and B_4C filled C–C composite discs were a 2D C–C composite comprising T300-3K fibers in an 8-harness satin weave, densified to ~1.5–1.6 g cm^{-3} by chemical vapor infiltration.

The ZrB_2 inhibited C–C composites followed a slightly different processing procedure as described herein. The T300-3K 8-harness satin weave fabric (TPI Style 4243) was dimensionally stabilized by heat-setting at high temperature in an inert atmosphere. Square fabrics (25.4 cm) were used for coating with precursor solution to zirconium diboride. Coated fabric was impregnated with a boron carbide filled phenolic resin, laminated, and autoclave cured. The cured panel was then processed first in an oven, then in a vacuum furnace, to convert the resin to carbon, and subsequently chemical vapor infiltrated to fill the voids with pyrolytic carbon. The finished panel had a thickness of 0.6 cm, a fiber volume of 47%, and a bulk density of 1.69 g cm^{-3}. The panel was cut into 1.6 cm diameter flat discs, which were used for further coating development and testing. All samples were cut at an angle to the plies to simulate a shingle lay-up.

Table 1
C–C composite compositions and physical properties.

Filler type	CC139C C-black	CCZrBC ZrB_2–B_4C	CC137E B_4C
CVD time (h)	150	150	150
Final density (g/cc)	1.593	1.637	1.695
Final voids (%)	16.7	16.3	16.2

The processing variables and purpose for pre-treatment are as follows: (1) filling the phenolic resin with B_4C particles will allow for the creation of a more oxidation resistant bulk C–C composites when an oxygen inhibitor, such as boron, is present within the composite. Inhibition of oxygen using B_4C particles increases the oxidation resistance of graphite.[5,20] The addition of ZrB_2 is believed to increase the high-temperature oxidation resistance above 1500 °C due to the more refractory oxide formations at temperature. The presence of B_4C inside the C–C weave also serves as a reservoir for boron that favorably interacts at high temperatures with carbon[5]; (2) chemical vapor infiltration (CVI) times of 150 were used in order to achieve high density materials.

2.2. ZrB_2 organometallic precursor

ZrB_2 precursor synthesis was conducted in the exclusion of air and water using standard glove box techniques under argon atmosphere. In order to synthesize precursors to ZrB_2 powders the following chemicals $ZrCl_4$, $NaBH_4$, and 1,2-dimethoxyethane (dme) were used. The appropriate concentration of $ZrCl_4$ was added to dme and stirred under an argon atmosphere. Then $NaBH_4$ was slowly added to the mixture followed by stirring for 12 h to allow for the simple exchange reaction to take place according to the following equation.[21]

$$ZrCl + 4NaBH_4 \xrightarrow{dme} NaCl + (Zr(BH_4))_4$$

At which point NaCl precipitated out of solution and was centrifuged for removal from the precursor suspension. The decanted $(Zr(BH_4)_4)$(dme) solution was then removed and underwent thermal treatment in order to confirm the formation of ZrB_2. Thermal heat treatments were performed under argon, using a 5 °C/min heating rate up to 1150 °C, hold for 1 h, and ramp down to room temperature at 20 °C/min. The formation of ZrB_2 nanoparticles was then confirmed using TEM and EDS analysis. This precursor synthesis has also been used to create ZrB_2 coated C–C composites.[22]

2.3. ZrB_2 sol–gel precursor processing

ZrB_2 synthesis was conducted in open-air environment inside a chemical hood. The following chemicals were used: zirconium oxychloride–hydrate, triethyl borate, and phenolic resin (~57% char yield) in anhydrous ethanol. A 30 wt.% solution of zirconium-oxychloride was prepared in ethanol by stirring overnight to fully dissolve the system. Triethyl borate (10 wt.% excess) and phenolic resin were then added to the solution and sonicated to fully dissolve the phenolic resin. The precursor

was then stirred for 2 h, and sonicated just prior to dip coating. The carbothermal reduction process took place within the C–C composites *in situ* at temperatures greater than 1100 °C and the process has been shown to be an endothermic process by the following reaction[23]:

$$ZrO_2 + B_2O_3 + 5C \rightarrow ZrB_2 + 5CO$$

2.4. Oxyacetylene torch testing: ablation and oxidation resistance measurements

A series of oxyacetylene torch tests were used to determine the ablation rates for the carbon black and UHTC filled C–C composites. Oxidation tests were carried out using an oxyacetylene torch test facility in observation with ASTM E 285-80.[24] Ablation rates were calculated as percent mass loss per unit time. The nozzle tip diameter is approximately 2 mm and the calculated heat flux of the combustion flame is approximately 418 kW/m^2, assuming no heat transfer losses. The emissivity was determined by a two-color radiation pyrometer and the surface temperature of the specimen was measured using a one-color pyrometer. The ablation rates for B_4C and carbon black filled C–C composites were measured at 800, 1000, 1200, and 1500 °C and were measured using a 900-s hold time at temperature. Ablation rates were also measured for unfilled and B_4C filled, and ZrB_2 and B_4C filled C–C composites at 1500 °C using a 300-s hold time at temperature.

2.5. Materials characterization

Polished cross-sections for the UHTC filled C–C composites were ground flat using 600 grit SiC papers then prepared with successively finer diamond abrasives to a 1.0 μm finish. Final polishing was achieved using a two-step process, starting with 0.3 μm alumina, then 0.04 μm silicon dioxide using vibratory polisher. The phase compositions of the ceramic filler material and unfilled C–C composites were analyzed with an X-ray diffractometer (Cu Kα radiation, X'Pert PRO, PANalytical, Almelo, The Netherlands) and a scanning electron microscope (SEM, Zeiss SUPRA 55VP FE-SE, Carl Zeiss SMT Inc., Peabody, MA) equipped with an energy-dispersive (EDS) X-ray microanalyzer. Transmission electron microscopy (TEM, Phillips, CM-30) was also performed in order to confirm the formation of ZrB_2 nanoparticles using the oganometallic precursor processing method. Solvent dispersed and dried nanoparticles were placed onto a carbon coated copper grid for morphological and EDS elemental analysis.

3. Results and discussion

3.1. Characterization of organometallic precursor derived ZrB_2 particles and ZrB_2–B_4C filled C–C composites

The formation of ZrB_2 nanoparticles from the borohydride precursor route was confirmed using TEM analysis, as seen in Fig. 1. The TEM micrograph shows that the nanoparticles are approximately 100 nm in diameter and that they are slightly agglomerated. The EDS spectra of the nanoparticles detected

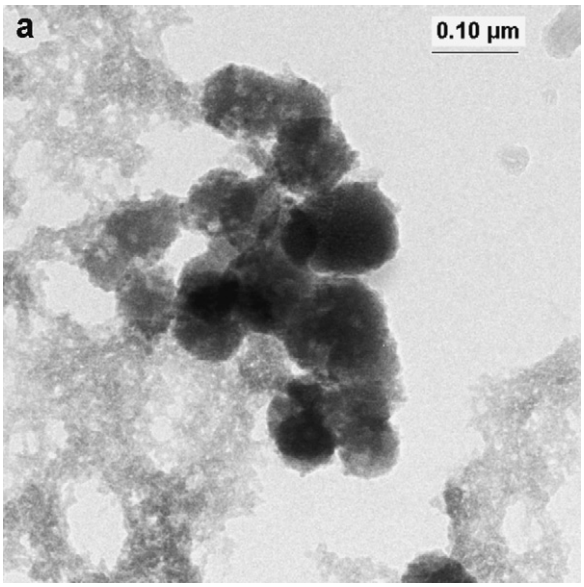

Fig. 1. Morphological of ZrB_2 nanoparticles synthesized from borohydride precursors shows the nanoparticle shape and size.

Zr and B due to the formation of ZrB_2 (not shown). Cross-sections for the ZrB_2–B_4C filled C–C composites are shown in Fig. 2. The dispersion of small ZrB_2 nanoparticles within the C–C composite is distributed throughout the composite cross-section (Fig. 2(a)) and throughout the bulk of the composite as seen in the back scatter contrast SEM image in Fig. 2(b). Based on quantitative image analysis it was approximated that the content of ZrB_2 particles within the C–C composites was ~0.3%. Fig. 2(a) also shows the detail of the C–C composite cross-section where the top CVD layer of graphite is on the surface, followed by a two-dimensional C fiber weave lay-up that is decorated with ZrB_2 particles.

Upon closer inspection, the ZrB_2 nanoparticles were detected within the B_4C filler material and they seem to fill the small void spaces in between individual C-fibers, as seen in Fig. 3. Furthermore, EDS analysis shows that the ZrB_2 filled C–C composites contain small nanoparticles composed of zirconium, as seen in Fig. 4. Furthermore, EDS maps of the ZrB_2–B_4C filled C–C composite cross-sections show Zr present throughout the composite (Fig. 5(a)) and XRD analysis detects ZrB_2 and B_4C filler material, and graphite from the composite (Fig. 5(b)).

3.2. High temperature oxidation behavior of B_4C filled and C black filled C–C composites

The oxyacetylene torch tests were used to measure ablation resistance for carbon black, B_4C and ZrB_2–B_4C filled C–C composites using the experimental set-up shown in Fig. 6. The detailed image of the test specimen (Fig. 6(b)) at temperature (1500 °C) is for a B_4C filled C–C composite and shows the evolution of a green colored gas that is expected to be boria gas, which is green in color. Ablation rates were measured for the carbon black filled C–C composites and B_4C filled C–C composites from 800 to 1500 °C (Fig. 7(a)). The ablation rate for the B_4C filled C–C composites is lower than the carbon black

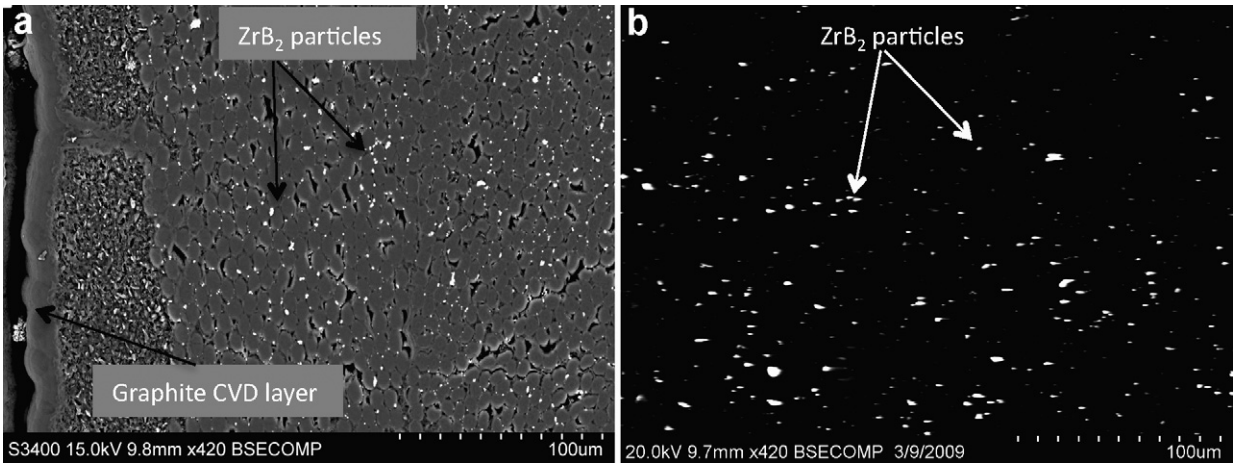

Fig. 2. SEM cross-sectional micrographs for ZrB_2 and B_4C inhibited C–C composites show (a) the CVD graphite layer and the distribution of ZrB_2 nanoparticles synthesized from borohydride precursors. (b) The high contract backscatter SEM micrograph highlights the ZrB_2 nanoparticles for use in area fraction calculations.

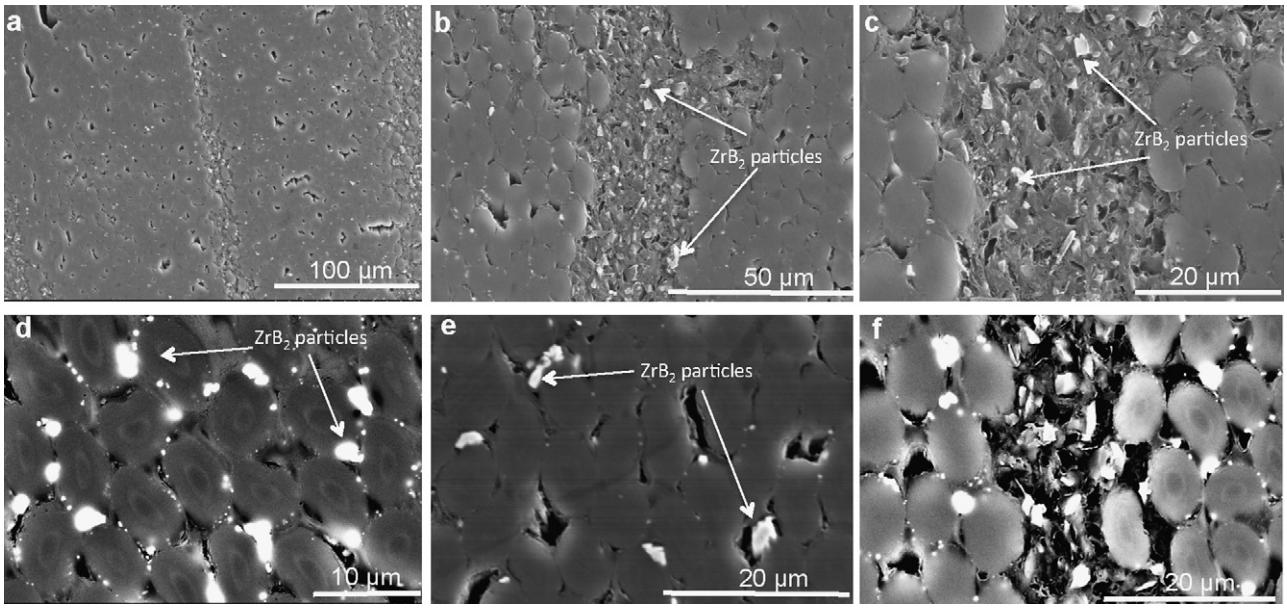

Fig. 3. SEM cross-sectional micrographs for ZrB_2 and B_4C inhibited C–C composites show the distribution of the B_4C filler material in between the C–C composite weaves (a–c). High resolution SEM micrographs show the distribution of fine ZrB_2 nanoparticles in between individual carbon fibers (d–f).

filled C–C composites from 800 to 1200 °C. At 1500 °C the B_4C filled composites show an increase in ablation rate most likely due to the rapid evaporation of liquid B_2O_3. The temperature dependence for lower ablation resistance at temperatures >900 °C can be explained based on the oxidation of B_4C into a glassy B_2O_3 that enhances oxidation resistance.[8] As the temperature increase then the vaporization of solid B_2O_3 to a gas phase increases and the ablation rates begin to increase and follows the uninhibited C–C composite ablation behavior. Therefore, B_4C filled C–C composites are slightly more ablation resistance than carbon black filled C–C composites from 800 to 1200 °C and show the potential to increase oxidation resistance at temperatures less than 1500 °C. Based on the preliminary results for B_4C inhibited materials it is favorable to have boron containing refractory particles within the composite that form the glassy B_2O_3 phases that inhibits the migration of oxygen into the substrate.

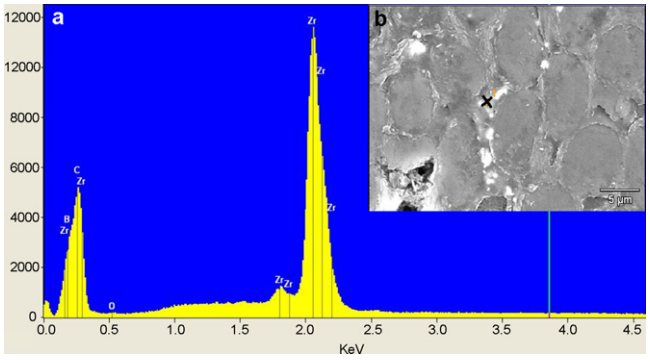

Fig. 4. EDS elemental analysis of ZrB_2 inhibited C–C composites shows the (a) detection of Zr, B, and O within the C–C composite (b).

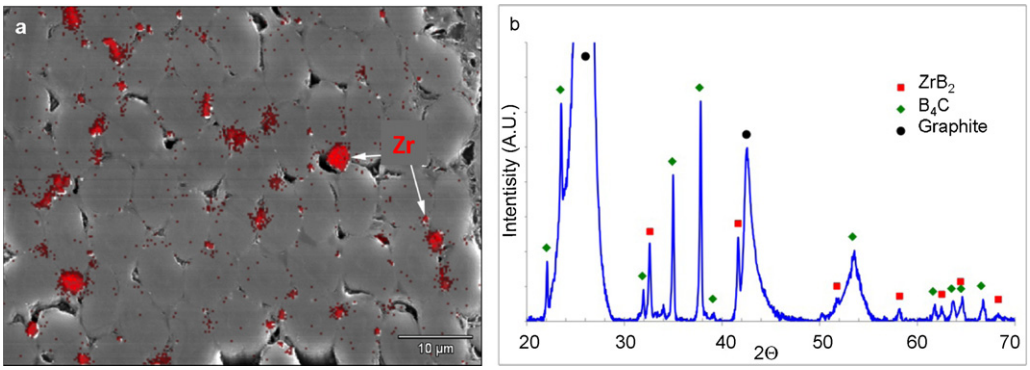

Fig. 5. The EDS elemental map of ZrB_2 inhibited C–C composites shows the (a) detection of Zr, within the C–C composite and (b) detection of ZrB_2, B_4C and graphite using XRD.

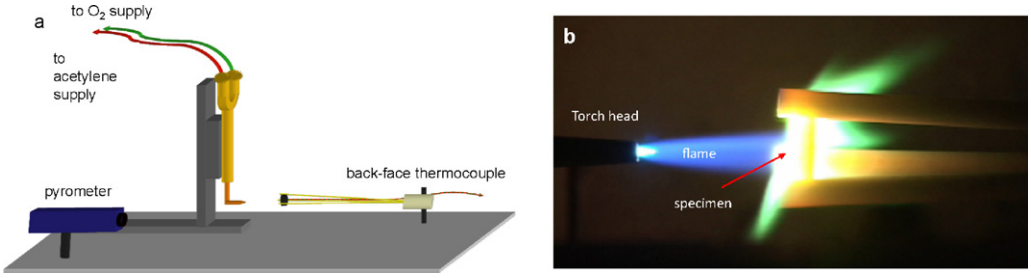

Fig. 6. (a) The oxyacetylene torch set-up used for measure ablation resistance of B_4C inhibited C–C composites and (b) an actual test specimen at temperature (1500 °C).

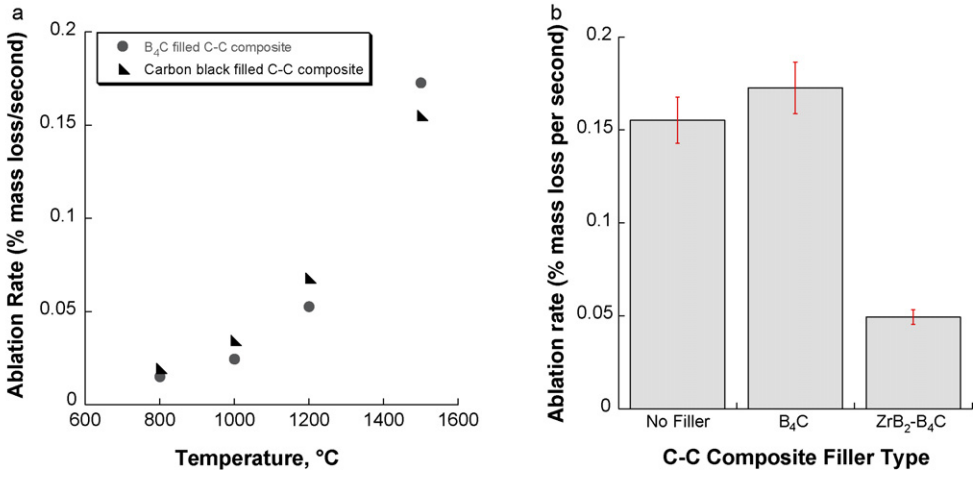

Fig. 7. Ablation rate measurements obtained using oxyacetylene torch tests for B_4C filled and carbon black filled C–C composites (a) from 800 to 1500 °C and (b) at 1500 °C for 300 s with ZrB_2–B_4C filled C–C composites.

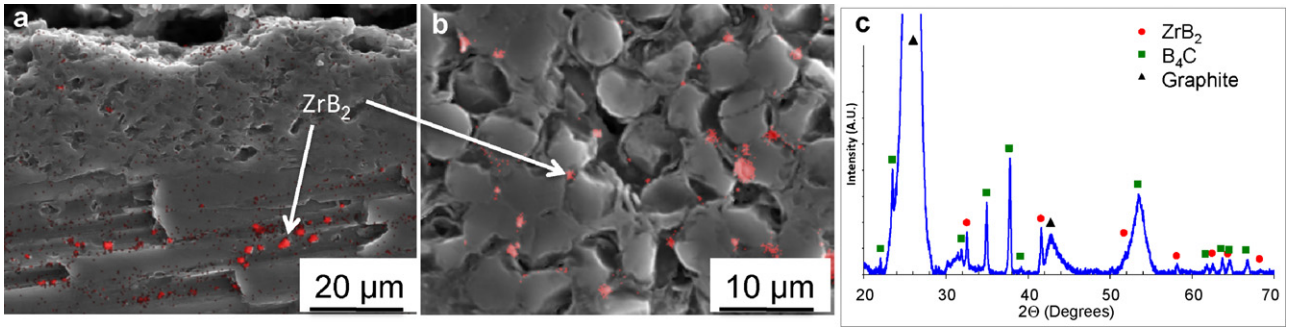

Fig. 8. SEM micrographs of ZrB_2–B_4C filled C–C composites after high temperature oxyacetylene torch testing at 1500 °C (300 s) in the (a) parallel direction and (b) perpendicular direction of the C–C composite weave structure and (c) XRD spectrum confirms the retention of ZrB_2–B_4C in the C–C composites after torch testing.

3.3. High temperature oxidation behavior of B_4C–ZrB_2 filled C–C composites

Ablation rates for carbon black, B_4C, and ZrB_2–B_4C filled C–C composites, at 1500 °C, are shown in Fig. 7(b). The ablation rate for the ZrB_2–B_4C filled C–C composite (0.0428) is 30% lower than the C-black (0.1552) and B_4C filled (0.1727) composites. Clearly, the inhibition of oxygen is increased using both ZrB_2 and B_4C particles as filler material in C–C composites. This is likely due to ZrB_2 having a higher melting temperature than B_4C and the ability to form high-temperature resistant oxides at temperature, such as ZrO_2. Upon oxidation of B_4C, the formation of liquid B_2O_3 promotes low temperature oxidation resistance and at higher temperature it couples with the formation of ZrO_2 and B_2O_3 from ZrB_2 oxidation in order to enhance the oxidation resistance of the C–C composite at temperature. The synergistic effect of ZrB_2 and B_4C oxidation over B_4C filled C–C composites can also be explained by the formation of a ZrO_2 oxide phase that limits the evaporation of B_2O_3 and increases the oxidation resistance at higher temperatures. The oxyacetylene torch tested ZrB_2–B_4C filled composites are shown in cross-section (Fig. 8). The microstructures show that ZrB_2 particles are still present throughout the bulk of the composite (Fig. 8). The EDS analysis detects Zr present in the composite from the filled ZrB_2 or the formation of ZrO_2. However, the X-ray diffraction spectra confirm that there are very little oxides present and the Zr elements are likely from the filled ZrB_2 particles (Fig. 8(c)). These preliminary torch-testing results will be used to design UHTC coating systems as ultra-high temperature oxidation protection materials on C–C composites and is the subject of a future publication.

3.4. Sol–gel derived ZrB_2 particles as an alternative method for processing ZrB_2 filled C–C composites

Based on the increased ablation rate resistance measured for ZrB_2–B_4C filled C–C composites we decided to investigate alternative approaches to incorporating refractory particles within the C–C composites using sol–gel precursors. This approach is very promising because the formation of ZrB_2 particles can easily be achieved within C–C composites at low temperatures (1150 °C). The XRD spectrum for the sol–gel material synthesized shows the formation of ZrB_2 and residual ZrO_2 that was not fully converted during the reaction (Fig. 9). Fig. 10 shows an individual carbon fiber coated with ZrB_2 nanoparticles that was processed using the carbothermal reduc-

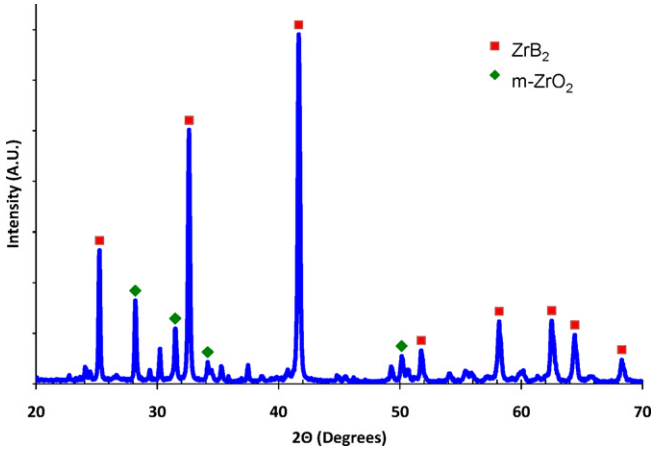

Fig. 9. The XRD spectra for ZrB_2 particles and residual ZrO_2 processed using the sol–gel precursor that was carbothermal reduced at 1150 °C.

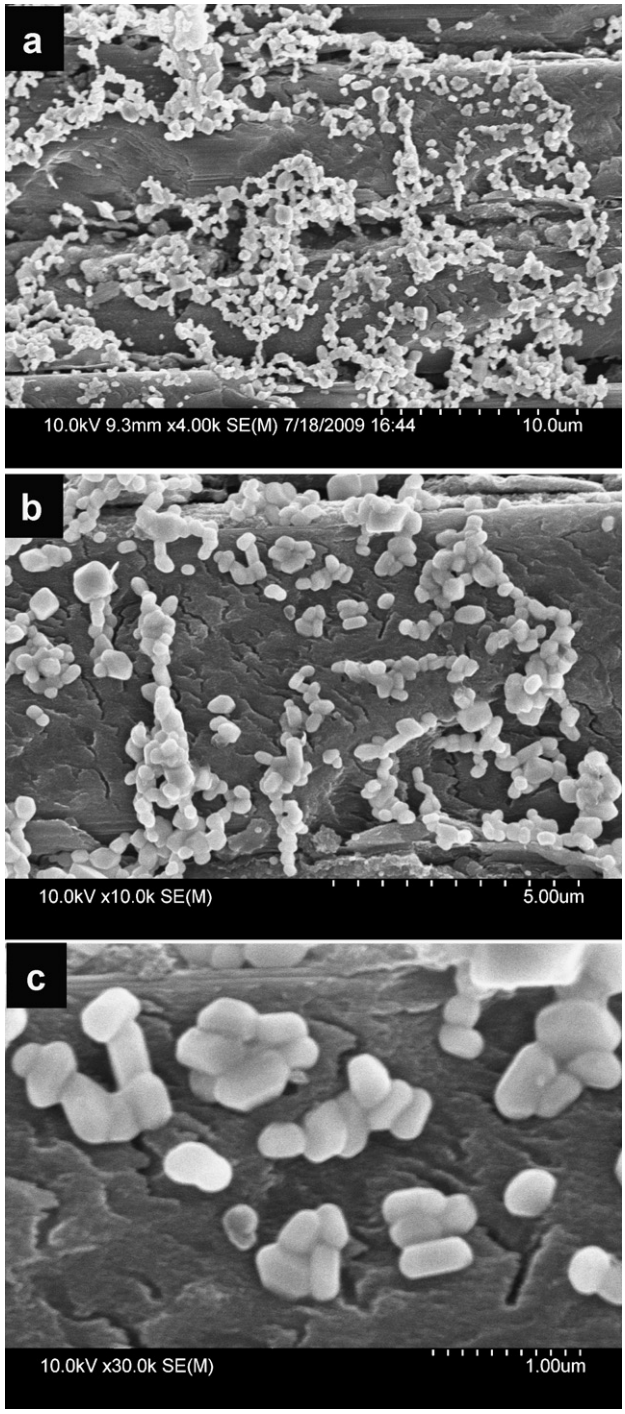

Fig. 10. SEM micrographs for ZrB_2 particles sitting on carbon fiber surfaces from (a) low to (b) medium to (c) high resolution that were successfully processed *in situ* at temperature within the C–C composite using the sol–gel precursor that was carbothermal reduced at 1150 °C.

tion method. EDS compositional maps show the detection of zirconium and oxygen containing particles on the carbon fiber surface (Fig. 11). The sol–gel precursor produces ZrB_2 particles with an average particle size of 300 nm and they are fine and equiax shaped particles. Preliminary results suggest that the carbothermal reduction temperature and time need to be optimized in order to obtain the full conversion of ZrB_2 but the formation takes place within C–C composites making it an ideal approach for inhibiting the oxidation of the composite at temperature.

3.5. Approaches for improved ablation resistant C–C composites

The approach we investigated in order to improve the oxidation resistance of C–C composites uses precursors to form UHTC particles within the composites and filling the weaves of the C–C composites with refractory particle fillers. The combination of refractory particle fillers can be optimized to achieve high temperature oxidation resistance without the use of external coating systems. However, if additional high-temperature oxidation protection is need a coating system can be incorporated into the process. The novel aspect of this work highlights the ability to combine refractory particles within the weave structure of the C–C composites during the lay-up and processing of bulk C–C composites. The refractory particles are homogeneously dispersed throughout the composite matrix and the synergistic effect of two UHTC particles is better than one filler particle. Our results show that B_4C particle filler provides enhanced oxidation resistance over the conventionally filled carbon black composites but the combination of B_4C and ZrB_2 particle filled composite system improves ablation resistance by at least 30% at temperature (1500 °C). Clearly, this approach that combines using precursors to UHTC to fill C–C composites has the potential to be used in extreme aerospace applications where high-temperature conditions are commonly experienced.

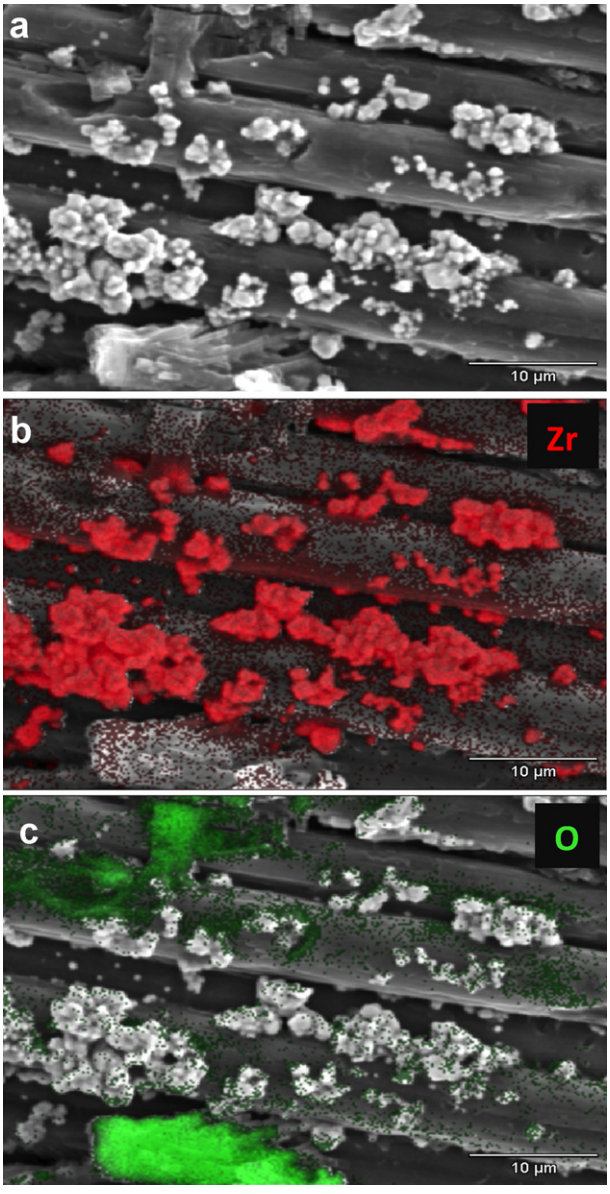

Fig. 11. SEM micrographs for (a) ZrB_2 particles sitting on carbon fiber surfaces and corresponding EDS elemental maps for (b) Zr and (c) residual oxygen in order to confirm the detection of ZrB_2 and ZrO_2 containing particles within the C–C composites using the sol–gel precursor method.

4. Summary

We have successfully processed C–C composites filled with ZrB_2–B_4C particles in order to increase the ablation resistance over conventional C–C composites by 30% at high temperature (1500 °C). We also processed C–C composites filled with B_4C particles that exhibit an enhanced oxidation resistance over conventional carbon black filled C–C composites from 800 to 1500 °C. Ablation rates were measured using an oxyacetylene torch test facility and the results suggest that this test method is very effective in evaluation high temperature oxidation properties for UHTC filled C–C composites. Overall, the ZrB_2–B_4C particle filled C–C composites were the most ablation resistant and our results suggest that the inhibition of oxygen migration to the bulk of the C–C composites is significantly enhanced using refractory filled composites. Thus, we also investigated alternative processing methods for filling C–C composites with ZrB_2 particles using sol–gel precursor processing methods. Preliminary processing methods seem to be very promising for use as a low cost approach for filling C–C composites and show that the ZrB_2 particles form within the C–C composites at low temperatures (1150 °C).

Acknowledgments

Author thanks and Ronald E. Loehman, formerly of Sandia National Laboratories, for technical assistance. Heat treatment of ZrB_2–B_4C filled C–C composites performed by Mr. Sam Lee of HITCO, Inc. is also greatly appreciated.

References

1. Levine S, Opila E, Halbig M, Kiser J, Singh M, Salem J. Evaluation of ultra-high temperature ceramics for aeropropulsion use. *J Eur Ceramic Soc* 2002;**22**(14–15):2757–67.

2. Sheehan JE. Oxidation protection for carbon fiber composites. *Carbon* 1989;**27**(5):709–15.
3. Sheehan JE. High-temperature coatings on carbon fibers and carbon–carbon composites. In: Buckley JD, Edie DD, editors. *Carbon–carbon materials and composites*. Norwich: William Andrew Inc.; 1993. p. 223–66.
4. Fitzer E. The future of carbon–carbon composites. *Carbon* 1987;**25**(2):163–90.
5. McKee DW. Oxidation behavior and protection of carbon–carbon composites. *Carbon* 1987;**25**(4):551–7.
6. Fahrenholtz WG. The ZrB_2 volatility diagram. *J Am Ceramic Soc* 2005;**88**(12):3509–12.
7. Gasch M, Ellerby DT, Johnson SM. Ultra high temperature ceramic composites. In: Bansal NP, editor. *Handbook of ceramic composites*. USA: Springer; 2005. p. 197–224.
8. Thevenot F. Boron carbide—a comprehensive review. *Euro-Ceramics* 1989;**2**.
9. Li, Shi, Zhang, Zhang, Guo, Liu. Effect of ZrB_2 on the ablation properties of carbon composites. *Mater Lett* 2006;**60**(7):892–6.
10. Shu-Ping L, Ke-Zhi L, He-Jun L, Yu-Long L, Qin-La Y. Effect of HfC on the ablative and mechanical properties of C–C composites. *Mater Sci Eng A* 2009;**517**(1–2):61–7.
11. Blum Y, Marschall J, Hui, Young. Thick protective Uhtc coatings for SiC based structures: process establishment. *J Am Ceramic Soc* 2008;**91**(5):1453–60.
12. Kern K, Gadow R. Liquid phase coating process for protective ceramic layers on carbon fibers. *Surf Coat Technol* 2002;**151**:418–23.
13. Pavese M, Fino P, Badini C, Ortona A, Marino G. HfB_2/SiC as a protective coating for 2-D Cf/SiC composites: effect of high temperature oxidation on mechanical properties. *Surf Coat Technol* 2008;**202**(10):2059–67.
14. Guo M, Shen K, Zheng Y. Multilayered coatings for protecting carbon–carbon composites from oxidation. *Carbon* 1995;**33**(4): 449–53.
15. Smeacetto F, Ferraris M, Salvo M. Multilayer coating with self-sealing properties for carbon–carbon composites. *Carbon* 2003;**41**(11): 2105–11.
16. Smeacetto F, Salvo M, Ferraris M. Oxidation protective multilayer coatings for carbon–carbon composites. *Carbon* 2002;**40**(4):583–7.
17. Marschall J, Pejakovic DA, Fahrenholtz WG, Hilmas GE, Zhu S, Ridge J, Fletcher DG, Asma CO, Thomel J. Oxidation of ZrB_2–SiC ultrahigh-temperature ceramic composites in dissociated air. *J Thermophys Heat Transfer* 2009;**23**(2):267–78.
18. Li G, Han W, Zhang X, Han J, Meng S. Ablation resistance of ZrB_2–SiC–AlN ceramic composites. *J Alloys Compd* 2009;**479**(1–2): 299–302.
19. Han J, Hu P, Zhang X, Meng S, Han W. Oxidation-resistant ZrB_2–SiC composites at 2200 °C. *Compos Sci Technol* 2008;**68**(3–4):799–806.
20. McKee DW. Borate treatment of carbon fibers and carbon/carbon composites for improved oxidation resistance. *Carbon* 1986;**24**(6):737–41.
21. Jensen JA, Gozum JE, Pollina DM, Girolami GS. Titanium, zircounium, and hafnium tetrahydroborates as "tailored" CVD precursors to metal diboride thin films". *J Am Chem Soc* 1986;**110**(5):1643–4.
22. Corral EL, Loehman RE. Ultra-high temperature ceramic coatings for oxidation protection of carbon–carbon composites. *J Am Ceramic Soc* 2008;**91**(5):1495–502.
23. Yan Y, Huang Z, Dong S, Jiang D. New route to synthesize ultra-fine zirconium diboride powders using inorganic–organic hybrid precursors. *J Am Ceramic Soc* 2006;**89**(11):3585–8.
24. ASTM E 285-80. *Standard test method for oxyacetylene ablation testing of thermal insulation materials*. ASTM International; 2002.